On the ocean salinity stratification observed at the eastern edge of the equatorial Pacific warm pool

C. Maes

On the ocean salinity stratification observed at the eastern edge of the equatorial Pacific warm pool

Christophe Maes[1]

Received 18 April 2007; revised 4 October 2007; accepted 19 December 2007; published 26 March 2008.

[1] The observations collected during a series of three oceanographic cruises dedicated to the study of the frontal zone at the eastern edge of the equatorial Pacific warm pool are used to study the role of salinity in the static stratification of the ocean upper layers. By combining physical and biogeochemical data, the position of the frontal zone at the surface could be accurately determined between 157.5°E and 173.4°E. A multiparameter approach is required due to the uncertainty that may result when one parameter is only considered. In the subsurface the thermohaline structures around the frontal zone reveal the predominant role of the ocean salinity stratification within the isothermal layers. However, the actual methods to determine the salinity barrier layer thickness cannot separate in detail the different dynamical regimes near the frontal zone and another variable to identify the role of the salinity in the static vertical stratification is then proposed and tested on several data sets. This method takes into account the thermal and the saline dependencies in the Brunt-Väisälä frequency in order to isolate the specific role of the salinity stratification in the layers above the main thermocline. The results show that the equatorial western Pacific is characterized by an increasing east-west gradient in salinity stratification whereas the stronger values are found westward of the eastern edge of the warm pool. This diagnostic then provides the basis for an examination of the dynamical mechanisms involved in the formation of the salinity stratification. It also confirms the importance of the ocean salinity in the variability of the equatorial Pacific warm pool. The potentially important implications for the El Niño-Southern Oscillation variability are discussed.

Citation: Maes, C. (2008), On the ocean salinity stratification observed at the eastern edge of the equatorial Pacific warm pool, *J. Geophys. Res.*, *113*, C03027, doi:10.1029/2007JC004297.

1. Introduction

[2] The upper waters of the equatorial Pacific Ocean can be divided into two regions, each having specific dynamical as well as biogeochemical characteristics and distinct ecosystem dynamics. In the central and eastern part of the basin there is an equatorial upwelling system with relatively cold and salty waters leading to a so-called High Nutrient-Low Chlorophyll (HNLC) status where the primary production and the biological pump interfere with the global carbon budget [*Inoue et al.*, 1996; *Le Borgne et al.*, 2002]. In the western part of the basin, there is a warm pool system characterized by warmer, fresher, and oligotrophic waters. The frontal zone separating these two regions of different oceanic properties is marked as well by a convergence of current at the eastern edge of the warm pool [*Picaut et al.*, 1996].

[3] From a physical point of view, the interest in understanding the variability of the eastern edge of the warm pool finds its roots in the oscillatory nature of the El Niño-Southern Oscillation (ENSO) phenomenon. In their conceptual model, *Picaut et al.* [1997] place the eastern edge of the warm pool at the center of action for air-sea interactions and they show that the ENSO time-scale can be accurately determined by zonal oceanic advection. When they include the warm pool displacements in their linear forecast model, *Clarke and Van Gorder* [2001] show that their ENSO predictions are improved. It appears then to be crucial to determine the position of the warm pool and to understand the underlying physical processes that are involved in its formation and variability. Although it is not well defined by sea surface temperature (SST), the eastern edge of the warm pool can be located by the convergence of zonal currents [*Picaut et al.*, 1996; *Maes et al.*, 2004] and also by a well-defined zonal salinity front that is trapped on the equator [*Delcroix and Picaut*, 1998; *Picaut et al.*, 2001]. To the east of the front, trade winds enhance the evaporation generating high surface salinity, while to the west, heavy precipitation associated with warm SSTs results in low surface salinity, the two effects combining to reinforce the front where the water masses converge. The increasing number of salinity

[1]Institut de Recherche pour le Développement (IRD), Laboratoire d'Etudes en Géophysique et Océanographie Spatiales (LEGOS), UMR065-IRD/CNES/CNRS/UPS, Centre IRD de Nouméa, Nouméa cedex, New Caledonia.

0148-0227/08/2007JC004297

observations by autonomous floats deployed in the context of the Argo program and the promise of satellite-observed ocean salinity in the near future [*Lagerloef*, 2002], it would seem that the determination of the front position is a simple matter of measuring the sea surface salinity (SSS). However, some direct observations of the frontal properties at the eastern edge of the warm pool showed little evidence of a front in the salinity data, whereas other physical and biogeochemical fields clearly showed the presence of the front [*Eldin et al.*, 2004]. Although the front position was initially defined by a specific isotherm or isohaline [e.g., *Picaut et al.*, 1996, 2001], the experience of *Eldin et al.* [2004] underlines the difficulty of defining a complex region by a single parameter such as salinity. Such difficulties are also illustrated by a definition of the frontal zone that extends over several degrees of longitude by *Matsumoto et al.* [2004], thus avoiding the problem of defining an exact position of the eastern edge of the warm pool that fits for all the parameters under consideration (K. Matsumoto, personal communication). This approach also allows for a possible separation between the physical and the biological fronts [*Eldin et al.*, 1997; *Rodier et al.*, 2000].

[4] In order to study specifically the structure and dynamics of the frontal area at the eastern edge of the warm pool, a series of three oceanographic cruises, Frontalis 1–3, has been staged from the IRD center of Nouméa on the R/V Alis in April 2001, April 2004 and April-May 2005. Although these cruises have been carried out under different climatic conditions, from weak La Niña to weak El Niño conditions, at each time the frontal zone at the eastern edge of the warm pool has been unambiguously identified [*Eldin et al.*, 2004, 2005]. The eastern edge of the warm pool along the equator has been found close to 157.5°E, 173.4°E, and 165°E during Frontalis 1, 2 and 3, respectively. It should be noted that the position of the front for the third cruise is based on a preliminary analysis of the data [*Eldin et al.*, 2005]. These positions are however in agreement with the previous estimates established by *Maes et al.* [2004] during the period 1992–2001 and they underline the dominance of the large-scale interannual variability in determining the position of the warm pool system. It is also important to note that the positions of the eastern edge of the warm pool have been determined by a multiparameter approach where physical, biogeochemical and biological fields are considered together.

[5] The zonal displacements of the eastern edge of the warm pool in the equatorial band are not limited to the surface. Associated transports of mass and heat are known to be considerable and important within the ENSO context [*McPhaden and Picaut*, 1990; *Delcroix et al.*, 1992] where they provide the thermal memory of the system [*Neelin et al.*, 1998]. In the subsurface the convergence of currents also leads to the formation of a barrier layer between the bottom of the mixed layer and the top of the thermocline that is attributable to salinity stratification as first described by *Lukas and Lindstrom* [1991]. Initially thought to be one of the important factors regulating entrainment cooling in the heat budget of the western Pacific warm pool [*Godfrey and Lindstrom*, 1989], the barrier layer has been also found to play an important role in the zonal displacements of the warm pool [*Ando and McPhaden*, 1997; *Picaut et al.*, 2001]. This latter effect is due to the trapping of the downward momentum flux of the wind-forcing in shallow mixed layers that may enhance the advection of SST during periods of strong westerly wind bursts [*Maes et al.*, 2002]. Such an air-sea interaction also contributes to the formation and enhancement of the barrier layer through a complex mechanism that involves the tilting and shearing of the salinity stratification above the top of the thermocline [*Roemmich et al.*, 1994; *Cronin and McPhaden*, 2002]. To date, the importance of the barrier layer in the dynamics of the Pacific warm pool has been mainly studied with general ocean circulation models [*Murtugudde and Busalachhi*, 1998; *Maes et al.*, 1998, 2002, 2005; *Vialard et al.*, 1998, 2002; *Boulanger et al.*, 2001; *Lengaigne et al.*, 2002]. All of these numerical models, whether forced by observed fluxes or coupled with an atmospheric model, show that the greatest sensitivity of the warm pool is in the eastern frontal zone. Nevertheless, the precise role of the salinity barrier layer in this crucial region has not been analyzed directly due to the lack of in situ data.

[6] In this study, the observations collected during the oceanographic Frontalis cruises are used to describe and to identify the potential role of the salinity stratification that characterized the eastern edge of the equatorial Pacific warm pool. In this sensitive region where SSTs approach or even exceed 28°C, the threshold for deep atmospheric convection, it will be shown that the salinity stratification connects the surface layers down to the thermocline and is closely associated with the warmest SSTs that are observed westward of the eastern edge of the warm pool. Another definition of the salinity stratification will be proposed in order to take into account the complete role of the salinity field within the upper layers of the ocean. Section 2 describes the data sets used in this study as well as the methodology used to identify the impact of the salinity stratification. The observations collected during the Frontalis cruises are first analyzed and compared with each other in section 3. These results are then combined with additional data sets from other oceanographic cruises and from the autonomous floats of the Argo program. All of the results are then discussed within the context of the thermohaline structure of the equatorial Pacific warm pool. A summary and some conclusions are presented in the last section.

2. Data and Methodology

2.1. The Oceanographic Frontalis Cruises

[7] The Frontalis program is composed by three oceanographic cruises staged from the IRD center in Nouméa, New Caledonia, on the research vessel Alis in April 2001, April 2004 and April-May 2005. All the cruises began with a meridional section along 165°E, extending the series of oceanographic cruises started along this meridian in 1984. The 165°E section was followed by a zonal section along the equator in search of the eastern edge of the warm pool, westward or eastward of 165°E. The detection of the frontal zone was done by analyzing in real time the salinity and the partial pressure of CO_2 in seawater and by considering indirect estimates of the salinity variability derived from the TAO/TRITON data [*Maes and Behringer*, 2000]. Once the longitude of the front was detected, the survey traced a "butterfly" pattern in order to achieve a broad zonal and

meridional description of the front properties at a higher spatial resolution (from 0.5° to 0.33° whereas other stations were occupied every 1°). Along the equator the stations have been done respectively between 165°E and 155°E, between 165°E and 176°E, and between 161°E and 167°E during the Frontalis 1–3 cruises, respectively. More details may be found in the mission reports by *Delcroix et al.* [2002], by *Ganachaud et al.* [2006], and by *Maes et al.* [2006a].

[8] Conductivity-Temperature-Depth (CTD) casts were made with a Sea-Bird model 911+ CTD down to 500 or 600 m depth along the equator. Temperature and conductivity sensors were calibrated at the factory after each cruise and in situ sampling with 8-L Niskin bottles were used to estimate the salinity accuracy of the CTD casts while underway. It is generally found that the accuracy of the salinity is better than 0.005 below 200 m. The R/V Alis is also equipped with an RDI model BB-150 Acoustic Doppler Current Profiler (ADCP), which allows the determination of currents within the top 250 m with 8-m bins. The SST and SSS were continuously recorded by a hull-mounted Sea-Bird model SBE-16 thermosalinograph (TSG) that provided averaged estimates every minute. After the calibration, the TSG biases have been corrected using the CTD data at the surface. After such corrections, the RMS differences in salinity between the TSG and the CTD data vary between 0.01 and 0.04 for the different cruises (salinity computations are based on the PSS-78 scale). Additional parameters such as nutrients (including nitrate, nitrite and phosphate), chlorophyll *a*, partial pressure of CO_2, and mesozooplankton were also collected and analyzed. The reader is referred to the aforementioned reports for more details on these observations.

2.2. Complementary Sources of Data

[9] In order to put into perspective some results obtained with the Frontalis cruises some complementary data sets will be used. These include the CTD casts of the WEPOCS cruises [*Lindstrom et al.*, 1987] that have been extracted from the World Ocean Database 2005 [*Boyer et al.*, 2006]. The data from these cruises formed the basis of our knowledge of the role of the salinity barrier layer in the western Pacific Ocean in work done by *Lukas and Lindstrom* [1991]. During the WEPOCS cruises, two sections along the equator, approximately between 143°E and 150°E, were done in June 1985 and February 1986. These data provide a very interesting point of comparison because they were localized in the far western equatorial Pacific, westward of the eastern edge of the warm pool. The salinity stratification computed from these past and present CTD data will be also compared with a climatological estimation. The monthly profiles of temperature and salinity from the CARS climatology [*Ridgway and Dunn*, 2003] will be used. Although it is desirable to use individual profiles rather than averaged profiles to determine the depth of the mixed layer [*de Boyer Montégut et al.*, 2004], our interest here will focus on the seasonal variations rather than the absolute depth of the mixed layer. Only the equatorial section between 150°E and 180° will be considered. Finally, the profiles of temperature and salinity collected by the autonomous floats launched by the Argo program will be also used to give an overview of the salinity stratification along the equatorial Pacific Ocean during the period 2002–2004. The details concerning these data may be found by *Maes et al.* [2006b]. This large collection of profiles will provide a solid basis for estimating the statistical relationship between the salinity stratification and the surface fields SST and SSS.

2.3. Methodology for Determining the Salinity Stratification

[10] Because the ocean interacts with the atmosphere through its surface, features of the ocean upper layers have long received close attention. The mixed layer is usually defined as the uppermost layer characterized by quasi-uniform vertical structure in the various properties of seawater. Historically, the most common approach used to determine the mixed layer depth (MLD) is to apply a specific criterion to the temperature profile. Different criteria have been used and they have been generally of two kinds; either a fixed temperature threshold, for example a 0.5°C decrease from the surface value, or a specified temperature gradient. Because the vertical density gradient is directly proportional to the buoyancy force *Lukas and Lindstrom* [1991] used a density gradient criterion as a more reliable way of estimating the bottom of the mixed layer. This last approach is a de facto recognition of the potential importance of the salinity field in stabilizing the upper ocean. Nevertheless, specific choices for thresholds or gradients will vary from one study to another depending on the nature of the data and on the region. *Anderson et al.* [1996] provide a sampling of some recent MLD criteria in their Table 2.

[11] Regarding the salinity stratification, *Lukas and Lindstrom* [1991] define the barrier layer as the thickness of the layer between the bottom of the mixed layer and the top of the thermocline. They used a density gradient criterion of 0.01 kg m^{-4} to determine the MLD and a temperature gradient of 0.05°C m^{-1} for the top of the thermocline (the LL method in the following). The depths where these criteria are met are determined by working downward from the surface. This approach works well with CTD casts which have a high vertical resolution, but *Sprintall and Tomczak* [1992], because they were working with climatological profiles with a coarse vertical resolution, devised a different method (the ST method in the following). They define the MLD by a density difference from the surface value that is equivalent to a decrease in temperature. This method also accounts for both salinity and temperature effects in determining the MLD. They set the equivalent decrease of temperature to 0.5°C for the MLD and used the same value for the threshold of the isothermal layer. Both the LL and ST methods will be referred to as the standard methods in the following.

[12] Most often, the standard methods return similar estimates of the barrier layer thickness (BLT) but, differences larger than 20 m do occur for some profiles collected during the Frontalis cruises. Such differences suggest that it would be helpful to define another variable that would more consistently reflect the subtle impact of the salinity stratification above the depth of the main thermocline near the eastern edge of the warm pool. The proposed method will take advantage of the dependency of the Brunt-Väisälä frequency, $N^2(T, S)$, on both temperature and salinity. If the salinity is removed from the computation of N^2, the

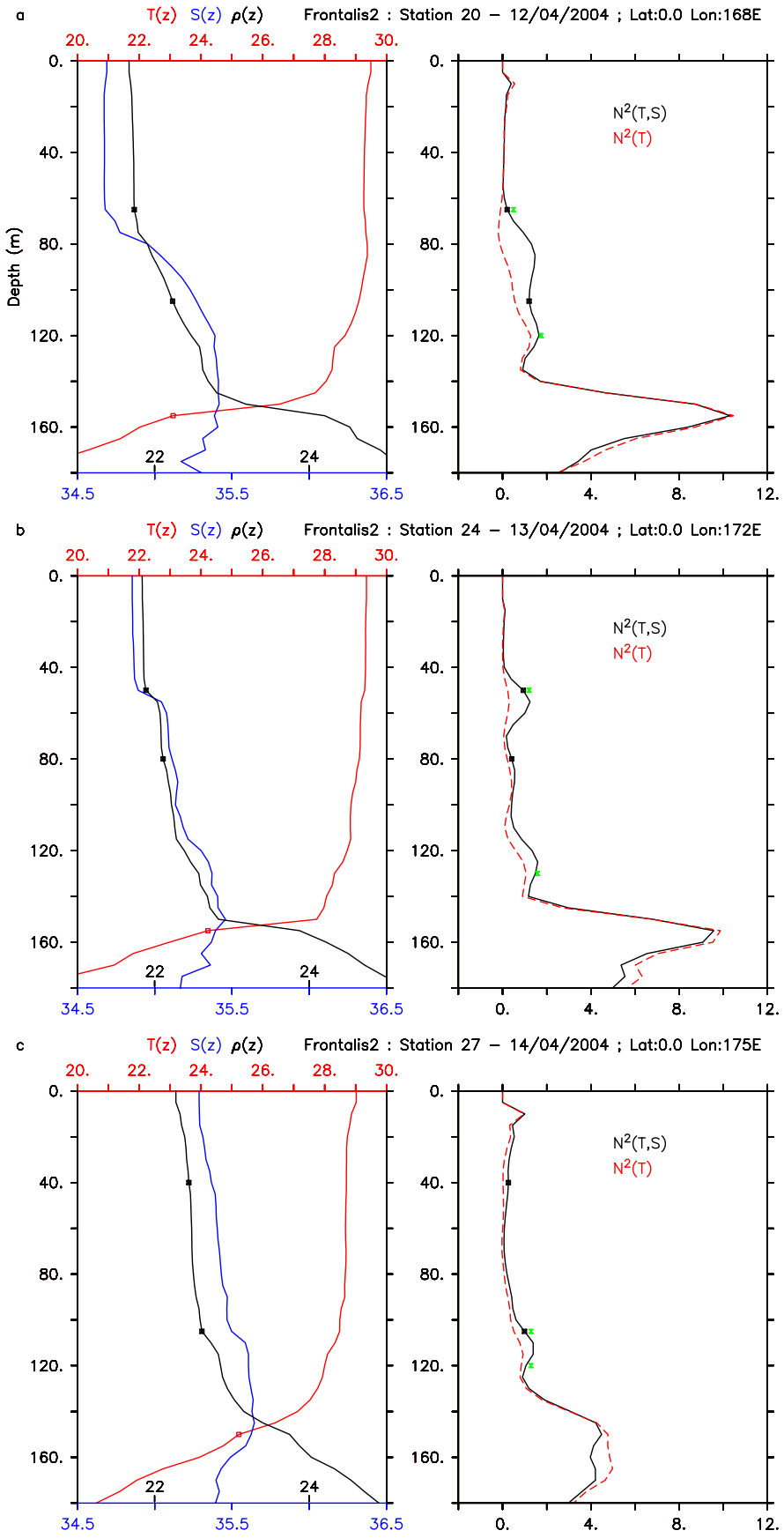
a
T(z) S(z) ρ(z)
Frontalis2 : Station 20 – 12/04/2004 ; Lat:0.0 Lon:168E
Depth (m)
N²(T,S)
N²(T)
b
T(z) S(z) ρ(z)
Frontalis2 : Station 24 – 13/04/2004 ; Lat:0.0 Lon:172E
N²(T,S)
N²(T)
c
T(z) S(z) ρ(z)
Frontalis2 : Station 27 – 14/04/2004 ; Lat:0.0 Lon:175E
N²(T,S)
N²(T)

Figure 1

result is a function of temperature alone, $N^2(T)$. By differencing the computation of N^2 that depends on temperature and salinity with the one that depends only on temperature, the layer where the salinity stratification has its greatest impact on N^2 can be isolated. For this study, all the temperature and salinity profiles are linearly interpolated to a constant 5-m vertical grid where the first level is defined at the 5 m depth, with the exception of the profiles provided by the Argo floats which are interpolated to the same grid using cubic spline functions. The top reference level of the computation is fixed at the 20-m depth to avoid variations confined near the surface, both in salinity and in temperature [*You*, 1995; *Shinoda et al.*, 1998]. The potential temperature and the density are both computed using the formulations of *Jackett and McDougall* [1995]. The computation of N^2 is based on the formulation proposed by *McDougall* [1987] where the coefficients of the salinity terms are zeroed out when computing the $N^2(T)$ profile. To reduce noise, a 15-m depth interval Hanning filter is applied to the temperature and salinity profiles before computing the N^2 profiles. The algorithm to estimate the salinity stratification is defined as follows: first, the depth of the thermocline is determined as the depth of the maximum value of the $N^2(T, S)$ profile. Second, two searches are made for the depths where the $N^2(T, S)$ and $N^2(T)$ profiles first diverge, one downward from the 20 m depth and one upward from the depth of the thermocline. The upper and lower depths determined in this way define the layer thickness where the strength of the salinity stratification is represented by the average value of the positive difference in the N^2 profiles. This quantity will be referred as the ocean salinity stratification (OSS) in the following.

[13] In order to illustrate some important differences between the OSS and the BLT, Figure 1 displays the vertical profiles of temperature, salinity, density, $N^2(T, S)$ and $N^2(T)$ for three stations observed during the Frontalis-2 cruise. In the first station the bottom of the isothermal layer is at 105 m, a depth that is 40 m deeper than the bottom of the mixed layer. This depth range is also characterized by a strong difference in the N^2 computations. It should be noted, however, that the difference between the N^2 functions extends farther down to the top of the thermocline near 120 m (as marked by the green symbols on Figure 1). This deeper extension of the barrier layer is also the result of the salinity stratification but it is not captured by the standard methods for computing the BLT due to masking by the temperature gradient. The second profile (Figure 1b) shows that, in a situation where the influence of the salinity stratification occurs in multiple layers, the overall size of the BLT could be underestimated by the standard methods. For this particular profile, the BLT computed by the ST method is 40 m larger than the BLT computed by the LL method. Finally, the third profile (Figure 1c) illustrates another drawback of the standard methods. In this case, the weak stratification that characterizes this profile allows for the threshold in the density gradient to be triggered at 40 m and the one in temperature to be triggered at 105 m. In comparison, the difference between the N^2 profiles is very small at these depths and the main jump in stratification of salinity near 110 m is missed by the standard methods. In this case, the difference between the LL and the ST methods is as large as 40 m, and the LL method appears to be more appropriate. Of course, the results of the standard methods for computing the BLT will be determined by the a priori choices for the threshold gradients used for both the density and the temperature. Small changes in the threshold values could greatly alter the results discussed above and that fact underlines the great sensitivity of the standard methods for computing the BLT.

[14] As noted earlier, the frontal zone during the Frontalis-2 cruise has been identified near 173°E, i.e., at a longitude between stations 24 and 27 (Figure 1). It is between these two stations that the differences between the standard methods for determining the BLT are the largest. At worst, the sign of the zonal gradient of the magnitude of the BLT across the eastern edge of the warm pool could be reversed depending on the method or depending on the assigned threshold values. On the other hand, using the difference between the N^2 profiles presents a potentially less ambiguous way to identify the impact of the salinity stratification above the main thermocline. It should also be noted that the new method proposed here provides a complementary measure of the importance of the salinity stratification.

3. Results

[15] As noted earlier, the equatorial section has been sampled by the three Frontalis cruises undertaken during different large-scale climatic conditions. On the basis of data recorded by the TSG, the sharpest front in SSS (a 0.2 difference over less than 1 km) was observed during the Frontalis-2 cruise. *Eldin et al.* [2005] places the front at the eastern edge of the warm pool at 173.42°E and finds this choice supported in terms of both physical and biogeochemical properties. The corresponding equatorial sections of temperature, salinity and density along the vertical are displayed in Figure 2. As expected, the temperatures in the surface layers are warm, generally warmer than 28°C, and characterized by a weak east-west gradient. In the layer warmer than 29°C, some temperature inversions larger than 0.1–0.2°C are present, a feature that has been often observed in the warm pool region. The thermocline is found around 160–180 m depth where the temperature gradient is maximal around the 20°C isotherm (not shown). The largest values of salinity are found above the thermocline, between 120 and 160 m, with a maximum of around 35.6 near 175°E. In this region the whole upper layer is characterized

Figure 1. Vertical profiles of potential temperature, salinity, and density (left panels) and associated profiles of $N^2(T, S)$ and $N^2(T)$ (right panels) for three different stations occupied during the Frontalis-2 cruise in April 2004. Units are respectively in °C, kg/m^3 and s^{-2} (scaled by 10^{-4}). The bottom of the mixed layer and the bottom of the isothermal layer as computed following the criteria defined by the LL method are represented by the black symbols on the density and $N^2(T, S)$ profiles. The red square on the thermal profile indicates the position of the thermocline. The green symbols on the $N^2(T, S)$ profiles indicates the position of the OSS layer as defined in the text.

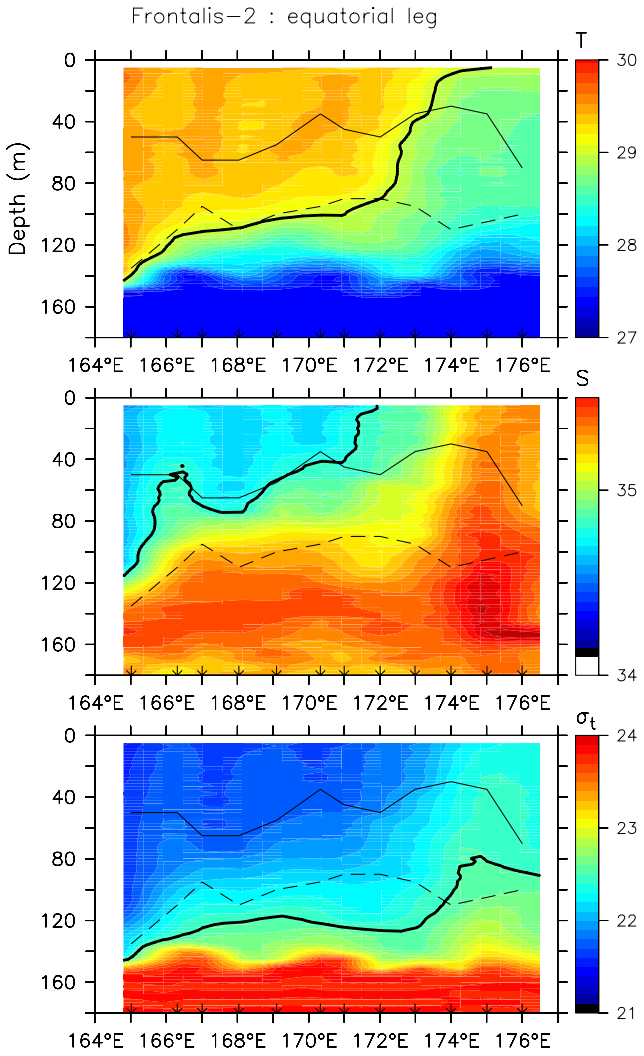

Figure 2. Vertical sections along the equator of potential temperature (°C), salinity and density (kg/m^3) as observed during the Frontalis-2 cruise in April 2004. The heavy black line respectively represents the 29°C isotherm, the 34.8 isohaline and the 22.5 kg/m^3 isopycnal, respectively. The thin and dashed lines indicate the bottoms of the mixed layer and of the isothermal layer (LL method). See the text for their precise definition. The arrows at the bottom of each panel indicate the position of the stations. Note that the temperature values below than 27°C are not represented.

by relatively high salinity values (larger than 35.2) that are close to their climatological values as compared with the CARS climatology. The extension of these waters toward the west only occurs above the depth of the thermocline but at approximately the same value of density (around 22.5 kg/m^3). In the upper layers low salinities around 34.4 are confined above the 22 kg/m^3 isopycnal and, as expected, the transition layer between the top of the thermocline and the bottom of the warm waters is characterized by strong salinity stratification.

[16] Superimposed on the vertical sections of Figure 2 are the depths of the bottom of the MLD and of the isothermal layer as defined by the LL method. The threshold criterion for the MLD has not been changed, but the threshold for the isothermal layer has been slightly increased (from 0.05 to 0.07°C/m) in order to avoid effects linked to weak and continuous temperature stratification as mentioned previously. Using these criteria the averaged MLD for the whole section is 48 m, which is deeper than previous estimates. It should be added, however, that the Frontalis-2 cruise took place during and after a relatively strong westerly wind burst (WWB) that probably deepened the MLD. The mean depth of the top of the thermocline is found to be 95 m at a position close to the depth of the 29°C isotherm along most of the section (Figure 2). As a consequence, a substantial BLT (larger than 40 m in average) characterized the equatorial section observed during the Frontalis-2 cruise. On average, an estimation of the BLT based on the ST method is found to be 41 m and it should be noted that both the bottom of the MLD and the top of the thermocline are deeper than were determined by the LL method. It means that these two estimates do not correspond strictly to the same part of the water column. However, by considering the OSS through its impact on the N^2 profiles, there is another story to tell. The equatorial sections of $N^2(T, S)$, $N^2(T)$, and their difference are displayed in the Figure 3. The largest values of the standard N^2 profiles are associated with the thermocline (Figure 1) at depths between 140 and 160 m (the maximum value for each profile is indicated by a star symbol on Figure 3). Above this depth the values decrease toward zero or near-zero values in the surface layers that are associated with the neutral or destabilizing conditions within the mixed layer. It should be noted that already an east-west difference in the N^2 profiles can be seen in Figure 3 at the depth of the barrier layer. By removing the salinity stratification in the N^2 computation, nothing is changed at the depth of the thermocline but important changes above the base of the isothermal layer are obvious. Finally, the differences between $N^2(T, S)$ and $N^2(T)$ shown in the bottom panel of the Figure 3 reveal a complex structure along the equatorial section. With the exception of a few negative values near the surface (above 20 m), such differences are always positive above the maximum of the $N^2(T, S)$ that will be identified as the depth of the thermocline hereafter in the text. To facilitate identifying where the N^2 differences are large, the depths where the value of 5×10^{-5} s^{-2} is found during the downward and upward searches by the OSS algorithm are indicated by solid and dashed lines. From east to west, three regions that exhibit different behaviors can be identified. East of 173°E, the differences are relatively weak and mainly localized in the vertical near their maximum values. Between 173°E and 170°E the differences are characterized by a double structure with large values at the bottom of the MLD and large values near or under the bottom of the isothermal layer. Finally, westward of 171°E the differences reach their maximal values at a depth that roughly corresponds to the center of the barrier layer. The N^2 differences of these three regions were also illustrated by the individual profiles shown in Figure 1. As will be discussed later the structure revealed in the differences in the N^2 profiles can be probably explained by different mechanisms at work in the formation of the barrier layer.

[17] Given the detailed structure of the OSS that can be seen in Figure 3, it is difficult to propose a single number to describe it all. Nevertheless, an advantage of the BLT definition is that it summarizes all the complexity of the

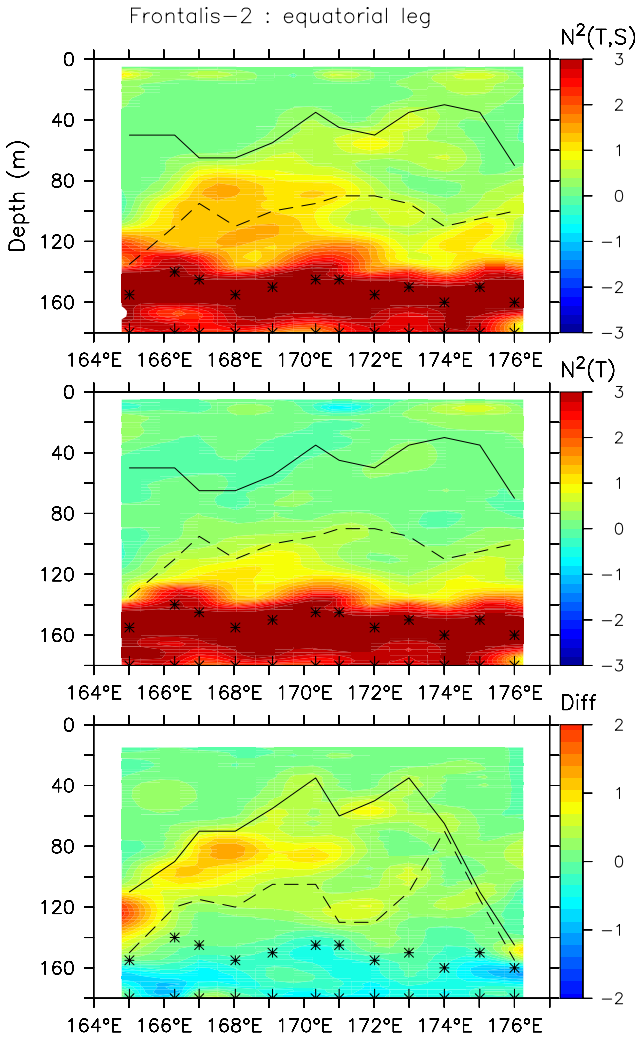

Figure 3. Vertical sections along the equator of N^2(T,S), N^2(T) and their difference (scaled by 10^{-4} s^{-2}) as observed during the Frontalis-2 cruise in April 2004. The star symbol represents the depth of the thermocline that has been defined as the maximum value of N^2(T, S). The thin and dashed lines indicate the bottoms of the mixed layer and of the isothermal layer in the two upper panels (LL method) whereas they represent the depths used to compute the OSS in the bottom panel. The arrows at the bottom of each panel indicate the position of the stations.

MLD and the thermocline depth in a single parameter. Obviously, a definition based on the OSS as a thickness layer that is confined between the bottom of the mixed layer and the top of the isothermal layer adds nothing new. Alternatively, the mean value of the OSS above the top of the thermocline will give some indications about the strength of the salinity stratification in the ocean upper layers. Figure 4 shows the OSS along the equatorial section during the Frontalis-2 cruise as well as the temperature and the salinity as defined by the algorithm as the surface level. Despite the coarse horizontal resolution as compared to the TSG data, it is evident that a frontal zone in temperature and salinity was crossed near 173°E. To the east of that zone, the OSS is weak, but to the west, it is characterized by a near linear, zonal gradient, increasing toward the west. The Figure 3 shows that the largest values of the OSS may be confined in a layer determined by the stronger difference values. The very thin layers are not however of interest because they may represent only a spiky value in the original profiles. When the thickness of the OSS layer is found to be less than 10 m, the N^2 difference is discarded in the resulting OSS computation. In such a case, Figure 4 shows that significant values occur only westward of the frontal zone, i.e., westward of 173°E. The largest values are reached in the far western part of the section, a result that may explain why high SSTs (>29°C) were maintained and not mixed with colder deeper water despite the occurrence of the WWB in this region.

[18] How these features of the OSS at the eastern edge of the Pacific warm pool differ from cruise to cruise allows an investigation of their robustness. Figures 5 and 6 show, respectively, the equatorial sections of temperature, salinity and differences in the N^2 profiles observed during the Frontalis-1 and the Frontalis-3 cruises, respectively. As the first cruise has been already described by *Eldin et al.* [2004] our attention here is focused directly on the OSS. Along the Frontalis-1 equatorial section, the depth of the isothermal layer is generally shallower than in the Frontalis-

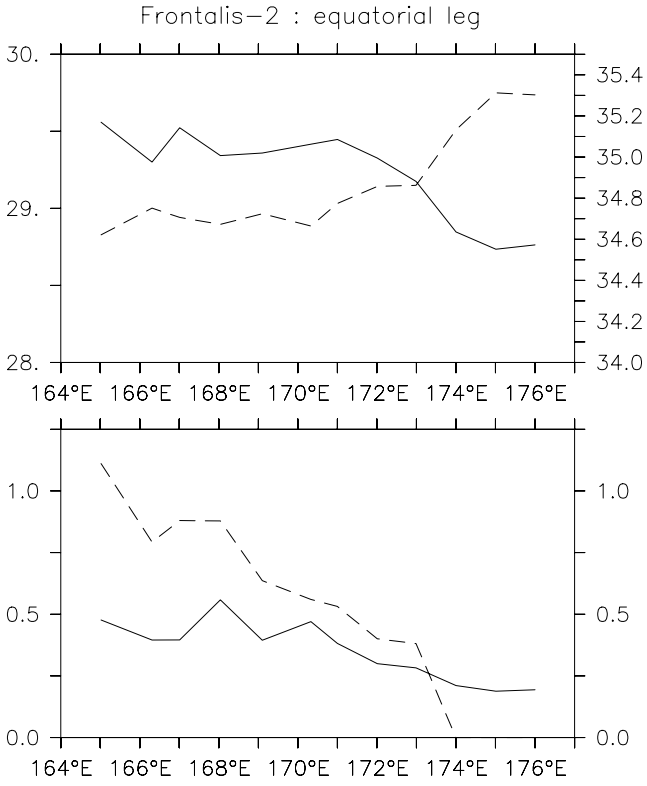

Figure 4. Observations of the potential temperature (°C) (solid line) and salinity (dashed line) values at 20 m depth (top) and of two OSS determination (bottom) along the equatorial section as observed during the Frontalis-2 cruise in April 2004. In the bottom panel, the thin line corresponds to the standard OSS computation whereas the dashed line corresponds to OSS values computed in layers determined by significant values of the N^2 difference (typically greater than 5. 10^{-6} s^{-2}).

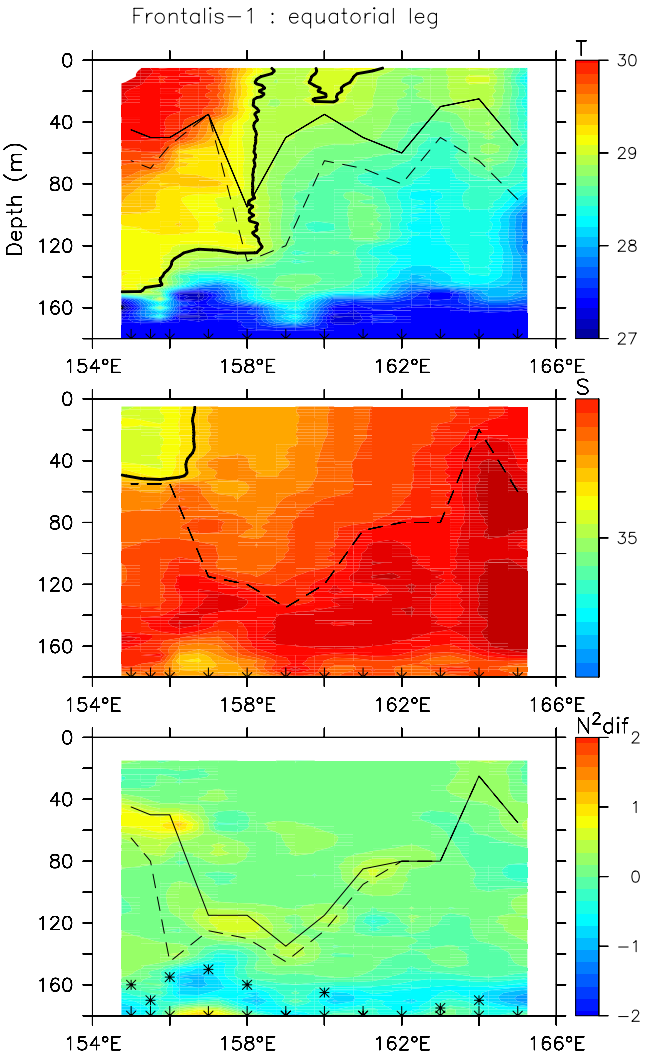

Figure 5. Vertical sections along the equator of potential temperature (°C), salinity and difference in N^2 (scaled by 10^{-4} s^{-2}) as observed during the Frontalis-1 cruise in April 2001. In the two upper panels, the heavy black line represents the 29°C isotherm and the 34.8 isohaline. In the upper panel, the thin and dashed lines indicate the bottoms of the mixed layer and of the isothermal layer (LL method). In the middle panel, the dashed line corresponds to the depth of the maximum gradient in salinity. In the lower panel the thin and dashed lines indicate the depths used to compute the OSS. The star symbol represents the depth of the thermocline that has been defined as the maximum value of N^2(T, S). The arrows at the bottom of each panel indicate the position of the stations.

2 section (Figure 2), but it should be noted that waters warmer than 29.75°C are observed from the surface down to 40–50 m, westward of 158°E. The presence of such very warm waters is not very unusual in the western equatorial Pacific [*Waliser*, 1996] and their maintenance is thought to be associated with a strong salinity barrier layer [*Delcroix and McPhaden*, 2002; *Maes et al.*, 2006b]. It is obvious from Figure 5 that the salinity of the upper layers was saltier almost everywhere as compared to Frontalis-2 and that the absence of a well-marked front is the striking feature of that cruise. The absence of a salinity front near the surface does not imply, however, the absence of a vertical salinity gradient in the upper layers. The position of the maximum vertical gradient in the salinity field above the thermocline is indicated by the dashed line in Figure 5 (middle panel). It shows, in particular, that the LL method will diagnose some non-negligible values of the BLT westward of 163°E. At approximately the same longitudes the N^2 profiles also exhibit some differences but they are weaker in amplitude and mainly confined to very thin layers. The stronger N^2 differences are found westward of 157°E and mainly localized near the 50 m depth. This latter result is thus consistent with the position of the frontal zone at the eastern edge of the warm pool diagnosed, mainly with biogeochemical parameters, by *Eldin et al.* [2004].

[19] During the Frontalis-3 cruise the thermocline was relatively shallow, at around 120 m, a situation that could be associated with the end of the weak El Niño conditions that prevailed at that time (the standardized index of the Southern Oscillation for the period March-April-May 2005 was equal to −0.8). Above the thermocline, warm waters occupied most of the equatorial section from 161°E to

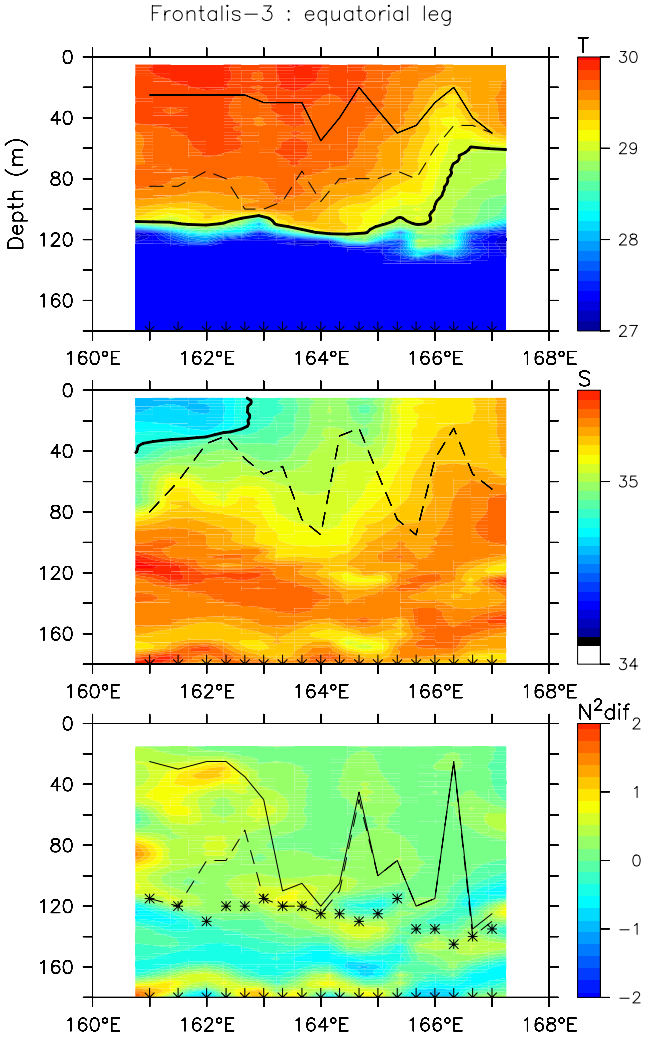

Figure 6. Same as Figure 5, but for the Frontalis-3 cruise in April-May 2005.

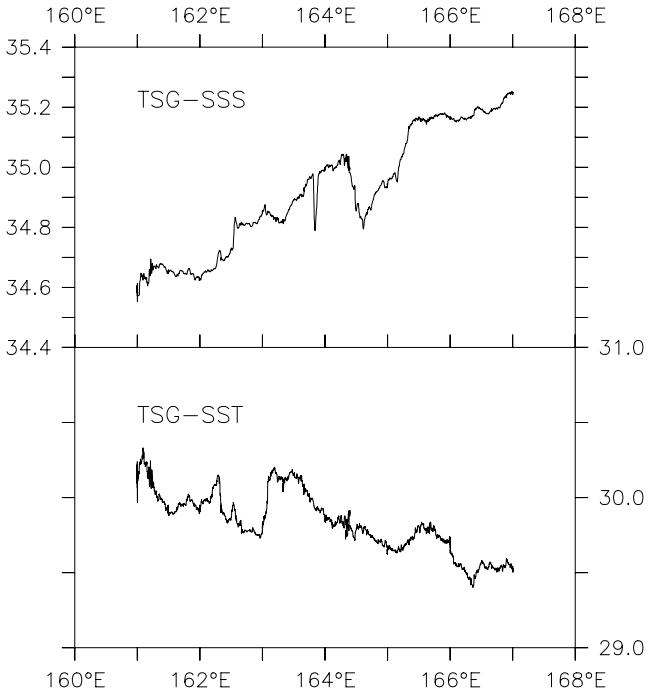

Figure 7. Continuous SSS and SST (°C) along the equator as observed by the thermosalinograph during the Frontalis-3 cruise in April-May 2005.

167°E and resulted in a strong thermal stratification near the 29°C isotherm (Figure 6). For this cruise, the bottom of the isothermal layer is at a similar depth if the original value for the criterion proposed by *Lukas and Lindstrom* [1991] is used (not shown). Similarly to the two other cruises significant BLT could be diagnosed along the whole section by the LL method. In the upper layers the salinity exhibits a strong gradient from the east to the west where the values decrease from 35.2 near 167°E to values less than 34.8 westward of 163°E. However, the frontal zone that separated these water masses is not as clearly defined as during the Frontalis-2 cruise. In this case, even the surface data of the TSG do not help to determine a clear front (Figure 7) due to the presence, in particular, of relatively low salinity values around 165°E. It is clear that, westward of these fresh waters, the SSS gradient is still decreasing and a secondary front, characterized by quite weak jump of 0.1, could be detected near 162.5°E. The SSS is always lower than 34.7 westward of that position. Returning to the vertical salinity structure illustrated in Figure 6, we see that such signals at the surface have a signature down to 40–50 m and that the depth of the maximum vertical gradient is characterized by displacements greater than 50 m. A similar "up and down" structure along the vertical is found in the depth boundaries of the OSS layer. The impact of the salinity stratification on the N^2 field appears to be significant only westward of 164°E, first near the depth of the thermocline and then closer to the surface, at the depth where the salinity is fresher than 34.8 (Figure 6). The latter suggests that the main front of the eastern edge of the warm pool, at least in terms of the physical parameters, should be between 163°E and 164°E, a position slightly westward of the preliminary estimation done by *Eldin et al.* [2005]. Another interesting feature observed during the Frontalis-3 cruise regards the closer proximity of the maximum differences in N^2 to the depth of the thermocline. Of course at these depths the total stratification is dominated by the thermal effect but it suggests, nevertheless, that the salinity may also participate in the total stratification in a non-negligible way. This point, which is not as clearly supported by the two other cruises, will be discussed in the next section.

[20] To complete the basic description of the OSS during the Frontalis-1 and -3 cruises, Figure 8 shows the OSS along the equatorial section in a way similar to the bottom panel of Figure 4 for the Frontalis-2 cruise. As might be expected the lowest values of OSS occurred during the Frontalis-1 cruise, but it should be noted that the section is still characterized by an east-west gradient increasing toward the far western Pacific. For the Frontalis-3 cruise a break in this gradient occurs between 164° and 165°E, but westward of that position, the amplitude of the gradient again increases and the largest values of OSS are comparable to the values reached a few degrees westward of the front as observed during the Frontalis-2 cruise (Figure 4). In each case the stronger OSS is associated with the presence of low salinity values in the surface layers and westward of the frontal region at the eastern edge of the equatorial Pacific warm pool. At depth, the stronger values of OSS appear near the base of the isothermal layer but strong values are also found down to the depth of the thermocline.

4. Discussion

[21] Like the standard methods for diagnosing the barrier layer, the OSS approach shows that the most important

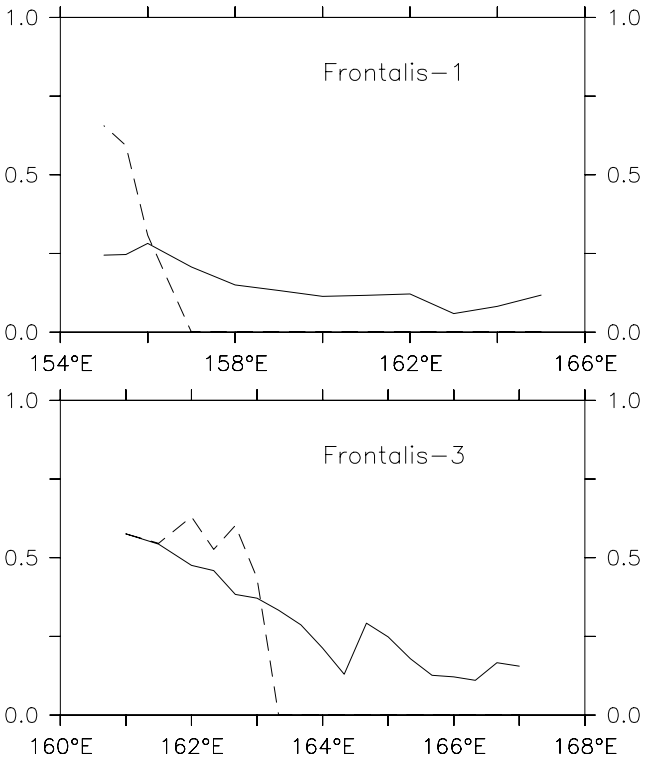

Figure 8. Same as the lower panel of Figure 4, but for the Frontalis-1 (top) and the Frontalis-3 (bottom) cruises.

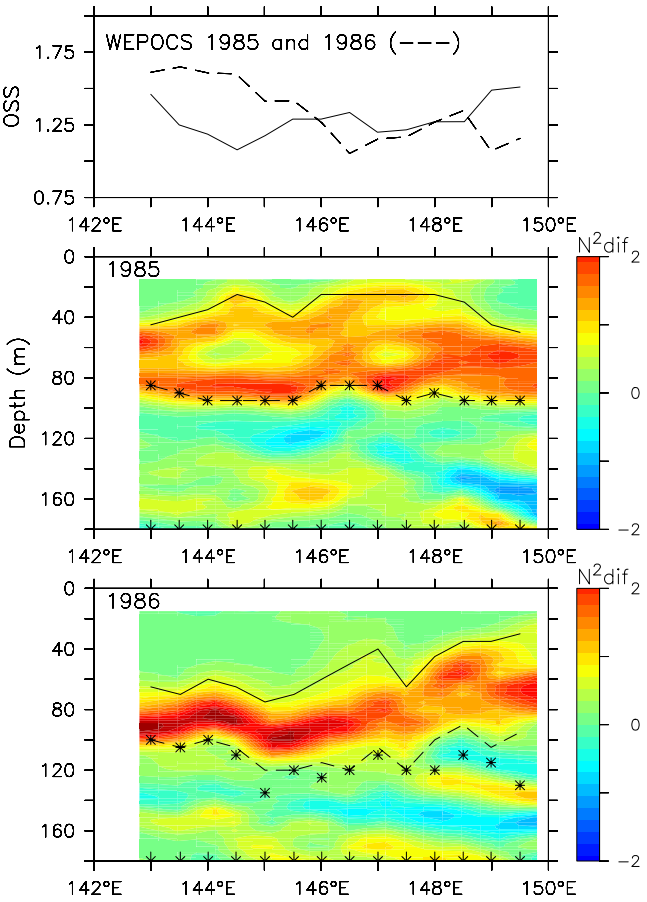

Figure 9. Equatorial section of the OSS observed during the WEPOCS-I (thin line) and WEPOCS-II (dashed line) cruises as well as vertical sections of the N^2 differences for the same cruises. In the lower panels, the thin and dashed lines indicate the depths used to compute the OSS. The star symbol represents the depth of the thermocline that has been defined as the maximum value of $N^2(T, S)$. The arrows at the bottom of each panel indicate the position of the stations.

impact on the static vertical stratification due to the salinity occurs westward of the front at the eastern edge of the Pacific warm pool. However, it also allows for a more detailed examination of the role of salinity within the warm waters (>28°C) of the western equatorial Pacific. This role was originally revealed by analyses of the CTD profiles from the WEPOCS cruises [*Lindstrom et al.*, 1987] and it is thus important to know how the two data sets compare each other. During the WEPOCS experiment the equatorial section was occupied twice, roughly between 143°E and 150°E, during June 1985 and during February 1986. These time periods were associated with the neutral or moderate La Niña conditions that prevailed after the strong 1982–83 El Niño event. As compared to the conditions during the Frontalis cruises, the depths of the thermocline were shallower, respectively between 80 and 120 m depth for the WEPOCS I and II cruises, respectively (Figure 9). It results in stronger salinity stratification mainly confined near the top of the thermocline throughout the equatorial section. Along the WEPOCS sections the salinity in the surface layer is fresher than during the Frontalis cruises (the depth of the 34.8 isohaline is 10- to 20-m shallower than the depth of the thermocline and surface values are around 34.2) and does not exhibit strong zonal variations, indicating that the front of the eastern edge of the warm pool was certainly somewhere east of 150°E. As a consequence the OSS exhibits strong values throughout the section with an east-west gradient that increases slightly toward the east in concordance with the gradient in SST (not shown). This is especially true during the WEPOCS I cruise. The OSS is also stronger in the upper layers during WEPOCS I as compared to the second cruise (Figure 9), which may be explained by the fact that WEPOCS II took place during a strong WWB [*Lukas and Lindstrom*, 1991]. Apart from having taken place under different interannual conditions, the WEPOCS cruises also differ from the Frontalis cruises by having occupied a section farther west and by having made their observations during different seasons. The latter issue could be investigated by considering the seasonal cycle of the OSS (Figure 10) deduced from the temperature and salinity profiles extracted from the CARS climatology [*Ridgway and Dunn*, 2003]. In the mean, the section between 150°E and 180°E is always characterized by a positive effect of the OSS that presents an east-west gradient increasing toward the west. The stronger values of OSS are mainly found westward of the 34.8 isohaline and exhibit a strong seasonal cycle that is maximum during the boreal winter period. The differences between the WEPOCS and the Frontalis cruises could be thus explained by a combination of the three aforementioned circumstances. It should be mentioned that the April-May period of time was chosen for the Frontalis cruises to ensure that the front at the eastern edge of the warm pool was not too far from 165°E, at least by seasonal time calculations, in order to match with the autonomous range of our R/V Alis.

[22] As shown with the Frontalis cruises the stronger values of the OSS allow an easier detection of the front at the eastern edge of the warm pool. However, oceanographic cruises represent a quasi-instantaneous snapshot of the

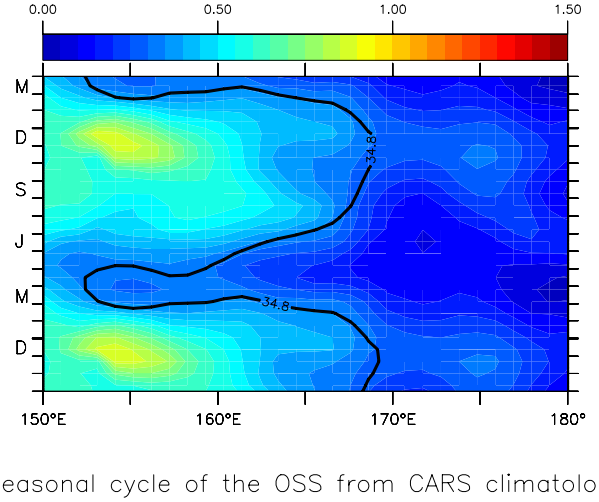

Figure 10. Seasonal cycle of the OSS (scaled by 10^{-4} s^{-2}) along the equator between 150°E and 180° as deduced from the CARS climatology. The thick black line represents the 34.8 isohaline.

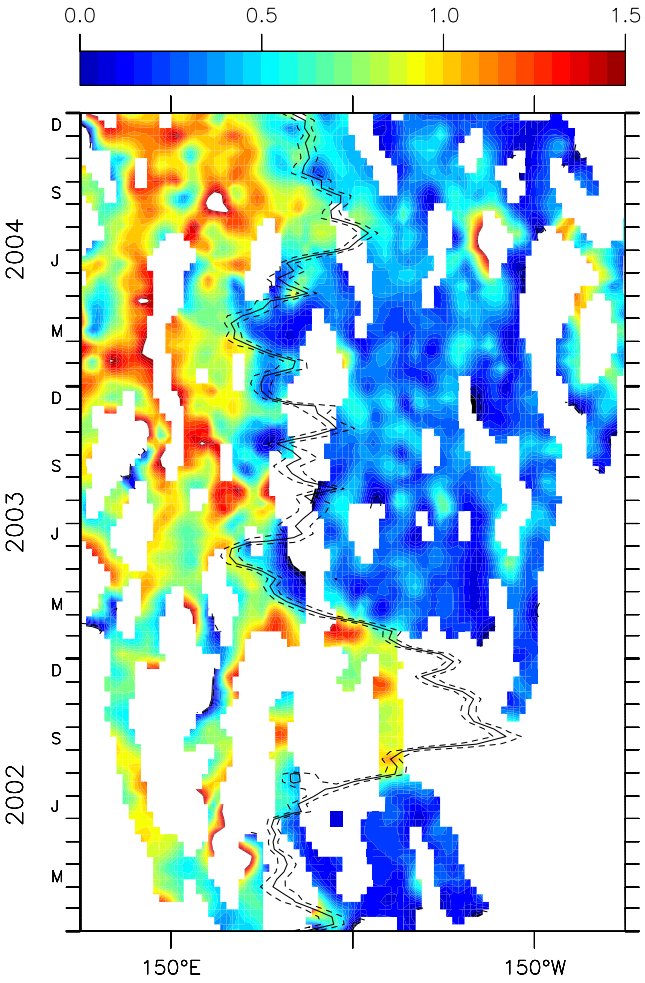

Figure 11. Longitude-time plot of the OSS (scaled by 10^{-4} s^{-2}) averaged for the 3°N–3°S band between 140°E and 140°W as computed from the temperature and salinity profiles collected by the Argo autonomous floats. The solid black line represents the 34.7 isohaline and the dashed lines indicate ± 0.2 around that value.

ocean and another approach is required to further test the usefulness of the OSS. Using the collection of profiles from the Argo project that have been already analyzed by *Maes et al.* [2006b], Figure 11 shows the longitude-time evolution of the OSS in the western Pacific Ocean over the period 2002–2004. Within the 3°N–3°S band it represents more than 2500 profiles of temperature and salinity and their associated estimation of the OSS. The stronger values in the OSS are essentially found westward of the dateline and their zonal extension varies in phase with the salinity front that indicates the eastern edge of the warm pool. Eastward of that front the OSS exhibits weak values. These different regimes could be distinguished in the scatter diagram of the OSS versus SSS as shown in the Figure 12. High values of SSS are associated with low values of OSS, typically less than one unit, but OSS values increase linearly as the SSS becomes fresher. For SSS lower than 34.2 it should be noted that the intensity of the OSS no longer increases but remains high. In Figure 12 both the WEPOCS and the Frontalis estimates of the OSS have been included and their separation shows that these cruises occurred under different physical regimes. The observations from the earlier cruises are characteristic of the far Pacific region while observations from the later cruises are associated with the front at the eastern edge of the warm pool. In contrast to the salinity diagram, a comparable diagram of OSS versus SST does not show the same partitioning of regimes (not shown). The Figure 11 could be compared to the Figure 2b from *Maes et al.* [2006b] and confirms that a broader region than just the vicinity of the eastern edge of the warm pool system is affected by a strong salinity stratification as reflected in the OSS. Furthermore, since strong salinity stratification restricts vertical mixing, the region where the OSS is large should be characterized by very warm SSTs and this turns out to be the case with high OSS values associated with SSTs typically greater than 29.75°C and by the presence of WWBs. The maximum values for the latter parameter are located about 10° of longitude west of the front. It thus reinforces the idea that operating within the equatorial warm pool region is a positive feedback loop involving the reduced vertical mixing (measured by the OSS), the fetch of westerly wind bursts and the warm SSTs. When this feedback loop is perturbed by disrupting one component, the reduction of the zonal extension of the warm pool could lead to the failure of El Niño as was demonstrated in coupled model experiments by *Maes et al.* [2002, 2005]. In these experiments the response of the model was analyzed in its normal configuration where the equation of state depends on temperature and salinity and in the second instance where it depends on only temperature. In other words, the experiments examined the results of canceling the impact of salinity stratification on ocean mixing in the warm pool. In the diagnostic terms of the present study, the standard measure of $N^2(T, S)$ was replaced by its $N^2(T)$ homologue. The OSS variability observed both at the seasonal and interannual timescales presented in this study provides some observational support for the variability imposed in these coupled model experiments. It also strengthens the argument that processes similar to those in the model experiments occur also in the natural system.

[23] If the impact of the OSS in coupled models is confirmed, then it is important to model development to understand the physical mechanisms involved in the formation and maintenance of the salinity structure and whether they function correctly in the models. On the basis of studies developed in the context of COARE, *Godfrey et al.* [1998] reported that zonal advection, meridional advection, as well as local forcing, and vertical mixing were all important for the maintenance and variability of the thermohaline structure in the Pacific warm pool. Away from the surface layers where rainfall plays an unquestionable role [*You*, 1995], two main mechanisms affect the three dimensional structure of the ocean and the formation of significant barrier layers. The original mechanism proposed by *Lukas and Lindstrom* [1991] hypothesizes the subduction of denser waters in the central Pacific below the lighter waters of the warm pool. This mechanism enhances the convergence of surface currents at the eastern edge of the warm pool [e.g., *Picaut et al.*, 2001]. The second mechanism is linked to the generation of velocity shear through a depth-dependent pressure gradient in the mixed layer linked to the zonal salinity gradient [*Roemmich et al.*, 1994]. *Cronin and*

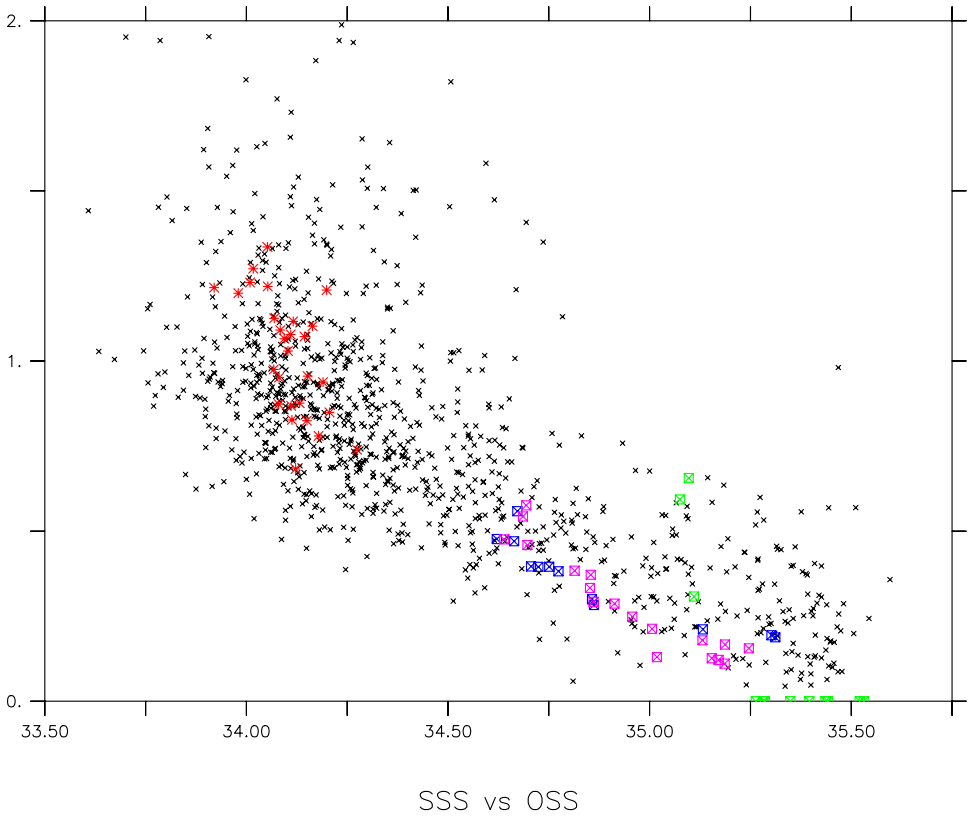

Figure 12. Scatter diagram of the SSS versus OSS (scaled by 10^{-4} s^{-2}) where the black crosses represent the values from the Argo autonomous floats, the colored squared symbols represent the Frontalis 1–3 cruises, and the red stars represent the WEPOCS-I and WEPOCS-II cruises.

McPhaden [2002] showed that this latter process could produce thick and long-lived barrier layers during WWBs. As discussed above the region where the OSS is strong (Figure 11) is also a region where the ocean's response to WWBs is strongest [*Maes et al.*, 2006b]. Briefly, a WWB will generate both an eastward Yoshida jet [*Yoshida*, 1959], and eastward propagating Kelvin wave. In the isothermal layer, the zonal salinity gradient accelerates the eastward flow increasing the vertical shear and causing a tilt of the isohalines toward the vertical. This formation of the vertical stratification due to the salinity will affect the BLT or the OSS. In the subsurface a westward current has been also observed to accompany some WWBs, a jet that may last and amplify after the wind event [*Richardson et al.*, 1999].

[24] ADCP currents measurements made during the Frontalis cruises offer an opportunity to compare the vertical structure of the zonal current with the OSS as shown in the Figure 13. At the depth of the thermocline the eastward current of 40–60 cm/s is the top of the equatorial undercurrent. Above this depth, the three cruises show different eastward and westward jets. The Frontalis-2 cruise takes place during and after a WWB that began at the end of March in the western Pacific and lasted approximately two weeks (westerly winds greater than 8 m/s had been observed by the TAO buoy at 165°E along the equator). The response was a strong eastward jet (>50 cm/s) above 100 m and a westward jet stronger than 40 cm/s beneath the surface jet (Figure 13b). Looking back at Figure 3, it can be seen that the layer characterized by the stronger velocity shear corresponds to the layer with the stronger OSS. These phenomena are of course correlated and this particular cruise shows that the tilting/shearing mechanism is able to form a strong OSS. The Frontalis-3 cruise takes place during a time of weak easterly winds (less than 4 m/s) but westward of 165°E and prior the cruise, a WWB occurred during the first three weeks of April (westerly wind around 8 m/s had been observed by the TRITON buoy at 147°E along the equator). As a consequence no surface eastward jet was observed along the equatorial section during Frontalis-3 and only a persistent westward subsurface jet, between 161° and 163°E, could be associated with this WWB. Here the stronger OSS (Figure 6) was observed well above the maximum of the westward jet and it may correspond to salinity stratification that was created prior the period of the Frontalis-3 cruise. It should be noted also that, above the stronger OSS in the surface layers, there is a convergence of currents just westward of the weak front detected in the TSG data (Figure 7).The current convergence has been typically observed a few degrees westward of the salinity front [*Maes et al.*, 2004] and this observation thus supports the idea of positioning of the eastern edge of the warm pool near 162.5°E. The situation during the Frontalis-1 cruise is different from the other cruises. As discussed by *Eldin et al.* [2004] the explanation for the patch of eastward current observed between 158° and 163°E is not obvious as moderate trade winds had been continuously present over the warm pool during the 3-month period before that cruise. The current might be related to some

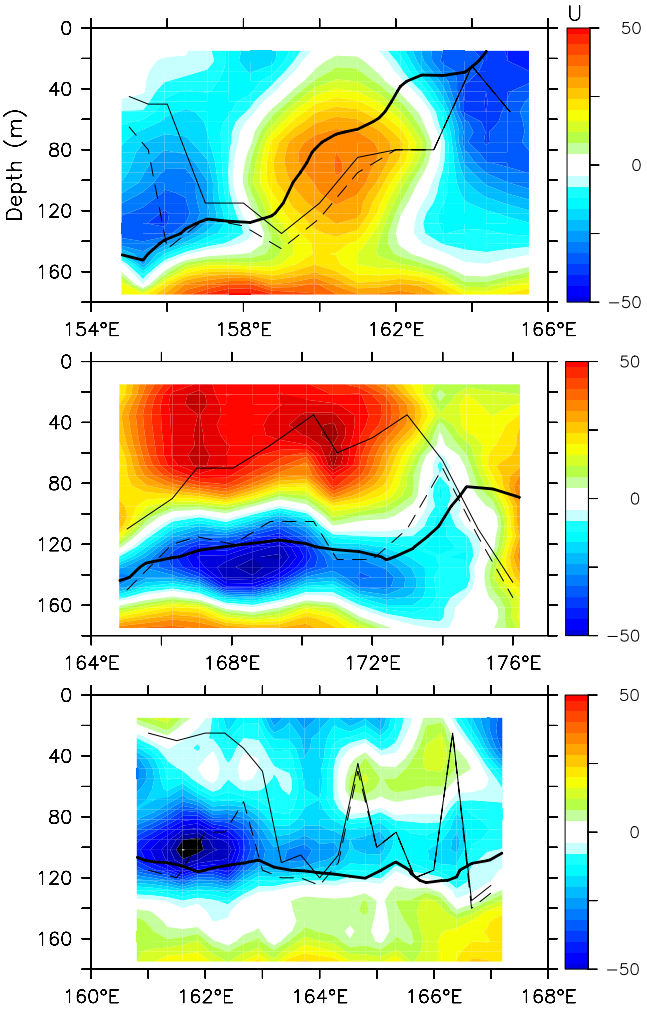

Figure 13. Vertical sections along the equator of zonal current (cm/s) as observed during the Frontalis-1 (top), Frontalis-2 (middle) and Frontalis-3 (bottom) cruises. The heavy black line represents the 22.5 kg/m^3 isopycnal. The thin and dashed lines indicate the depths used to compute the OSS.

observed OSS (Figure 5), but both the amplitude and the vertical scale of that salinity stratification are very weak. Another interesting feature is the uplifting of the density field toward the surface as represented by the position of the 22.5 kg/m^3 isopycnal in Figure 13. This isopycnal reaches the surface near 165°E where the SSS is around 35.5 and the SST is still above 28°C. These values are consistent with upper water masses from the central Pacific and they are close to the values of the CARS climatology. Assuming that the eastern edge of the warm pool is west of this position, this water mass might be regarded as likely to be subducted under the lighter waters to the west. On the other hand, the eastward current during the Frontalis-1 cruise would not favor subduction and, even in the absence of an eastward current, the resulting OSS would be quite weak as mentioned previously. In addition, the results from the Frontalis-2 and -3 cruises show that the subduction process probably does not form significant OSS near the eastern edge of the warm pool. Nevertheless, such a process should not be completely disregarded because oceanographic cruises can provide only snapshots of the ocean's structure. A more quantitative analysis of the different mechanisms involved in the formation of the OSS may have to rely on numerical models.

5. Summary and Conclusion

[25] The principal objective of the Frontalis cruises was to observe the eastern edge of the western Pacific warm pool where the warm and low salinity waters of the warm pool are in close proximity to the cold and high salinity upwelled waters of the cold tongue in the central-eastern equatorial Pacific. In this region where the SSTs are permanently above 28°C the eastern edge has been shown to be characterized by a sharp front in SSS that is trapped to the equator. This major feature has been observed to be associated with a sharp salinity front during the Frontalis-2 cruise, although a salinity front was much less evident during the other two cruises. As reported by *Eldin et al.* [2004] this canonical feature was not observed during the Frontalis-1 cruise but the analysis of the other observed parameters allowed an accurate determination of the position of the eastern edge of the warm pool. The position of that zone was also difficult to ascertain for the Frontalis-3 cruise where a double structure in the fresh surface waters could be misinterpreted.

[26] The zone of convergence on the eastern edge of the Pacific warm pool separates two water masses that extend well below the surface. This sharp separation of the water masses facilitates the formation of the salinity barrier layer in the isothermal layer of the warm pool. The resulting salinity stratification creates the barrier layer that is particularly effective in trapping heat and the momentum of the wind-forcing in the upper layers. However, standard approach for estimating the BLT, based on thresholds with pre-determined criteria, cannot identify variations in the strength of the salinity stratification within the Pacific warm pool. Because the dissipation of the density gradient is related to the strength of the static stability which can be measured by the Brunt-Väisälä frequency, another approach to diagnosing the strength of the barrier layer, based on N^2, has been proposed and tested with the data collected during the Frontalis cruises. By differencing $N^2(T, S)$ and $N^2(T)$ it is shown that the resulting field can reveal the importance of the salinity stratification that is associated, for one part, with the barrier layer. The new approach is also effective at capturing significant values of the salinity stratification at depths above the main thermocline.

[27] The determination of the ocean salinity stratification along the equatorial sections observed during the Frontalis cruises shows that the western equatorial Pacific is characterized by an east-west gradient where the larger values occur westward of the eastern edge of the warm pool. This maximum in the OSS corresponds to the preliminary identifications of the frontal zone based on a multiparameter analysis. For the particular case of the Frontalis-3 cruise the analysis suggests that the physical and the biogeochemical fronts are effectively separated, a situation that had been also observed in some previous cruises. Moreover, by using the temperature and salinity profiles from the Argo floats it was found that the eastern edge of the warm pool is

permanently characterized by a strong gradient in the OSS. This gradient in OSS usually varies in phase with the surface front in sea surface salinity. This point thus reinforces the argument that the salinity stratification plays a major role to the zonal movements of the eastern edge of the warm pool [e.g., *Picaut et al.*, 2001]. The convergence of zonal currents associated with the front of the eastern edge of the warm pool also seems to reinforce the idea that waters of the central Pacific are subducted below the waters of the warm pool. However, no clear evidence of such process was found during the Frontalis cruises. The vertical structure of the different jets associated with the salinity stratification suggests that it is more likely that the formation of the OSS results from a tilting and shearing process at the salinity front when the warm pool is displaced eastward. It remains possible, however, that both processes operate separately, for instance, in different parts of the central and western Pacific, and that they may be associated only under certain extreme conditions such as strong ENSO events.

[28] The front at the eastern edge of the warm pool is an essential feature of the ENSO coupled system in the central equatorial Pacific according to *Picaut et al.* [1997]. In this formulation the basic period of ENSO is closely linked to the eastward and westward displacements of the front. When the system is moving eastward it is assumed that the expansion of the warm waters and thus high SSTs occurs in concert with the fetch of the westerly winds. The intensity of these ocean-atmosphere interactions appear to be controlled in part by the ocean salinity stratification that obstructs entrainment of the cold deep water into the surface layer. The diagnostic that has been proposed in this study takes into account this particular effect without considering at all the thermal stratification above the main thermocline. The blocking of the effects of salinity stratification in a coupled numerical model led to the failure of model ENSO events to develop. This result was explained by *Maes et al.* [2002, 2005] as due to a weakening of the SST-wind stress relationship. The results of this present study support these conclusions through direct observational validation of model features. They also confirm the important role played by the salinity stratification as one of the mechanisms that are involved in the positive feedback loop within the ENSO theory proposed by *Picaut et al.* [1997]. Moreover, the Frontalis cruises revealed no clear relationship between the OSS and the SST that might be the result of local air-sea fluxes and therefore argues for a more careful treatment of salinity in ENSO models. Within the warm pool system, i.e., westward of the front, the OSS exhibits complex and non-stationary features (Figure 11), a result that is consistent with the analysis based on the thermohaline observations collected during COARE as reported by *Huyer et al.* [1997].

[29] In the next few years the number of profiles measuring the salinity in the ocean will increase by virtue of the Argo program and it is thus expected that the future studies combining observations and numerical modeling will more precisely establish of the role of the ocean salinity stratification within- and at the eastern edge of the equatorial Pacific warm pool. At present it is thought that salinity stratification is most important during the period prior to the onset of ENSO conditions. From this perspective it is essential that coupled models that are used in ENSO forecasts or in global change experiments should be able to reproduce these features. The definition of the OSS that has been proposed in this study is a simple diagnostic that ocean modelers could easily employ in their analyses and in the metrics that they use to validate their models.

[30] **Acknowledgments.** Special thanks to the officers and crew of the R/V Alis who operated the three oceanographic Frontalis cruises. Thierry Delcroix and Alexandre Ganachaud lead, respectively, the first and the second cruise. The large quantity of data collected during these cruises is also due to the active participation of the technicians, engineers and scientists involved in the Frontalis project that was lead by Thierry Delcroix. All these individuals are gratefully acknowledged. Some preliminary results that are included in this study were part of the training material of Jérôme Van Winsberghe in his master's program at the University of Marseille. The root encouragement for this study was generously provided by Billy Kessler during some discussions held at the Dynamic Planet conference in Cairns, August 2005. Comments from Dave Behringer, Christophe Menkes and one anonymous reviewer were greatly appreciated. The Frontalis data have been archived by the SISMER data center (www.ifremer.fr/sismer/). The Argo data are collected and made freely available by the International Argo Project and the national programs that contribute to it (www.argo.ucsd.edu, argo.jcommops.org). The tropical Pacific TSG database is maintained at the IRD center of Nouméa by David Varillon, as a part of the French ORE-SSS (www.legos.obs-mip.fr/observations/sss/). TAO/TRITON is a joint effort between PMEL and JAMSTEC (these data are freely available at www.pmel.noaa.gov/tao/ and www.jamstec.go.jp/jamstec/TRITON). This work is supported by the Institut de Recherche pour le Développement and, partially, by the Centre National d'Etudes Spatiales agency.

References

Anderson, S. P., R. A. Weller, and R. B. Lukas (1996), Surface buoyancy forcing and the mixed layer of the western Pacific warm pool: Observations and 1D model results, *J. Clim.*, *9*, 3056–3085.

Ando, K., and M. J. McPhaden (1997), Variability of surface layer hydrography in the tropical Pacific Ocean, *J. Geophys. Res.*, *102*, 23,063–23,078.

Boulanger, J.-P., E. Durand, J.-P. Duvel, C. Menkes, P. Delecluse, M. Imbard, M. Lengaigne, G. Madec, and S. Masson (2001), Role of non-linear oceanic processes in the response to westerly wind events: New implications for the 1997 El Niño onset, *Geophys. Res. Lett.*, *28*, 1603–1606.

Boyer, T. P., J. I. Antonov, H. E. Garcia, D. R. Johnson, R. A. Locarnini, A. V. Mishonov, M. T. Pitcher, O. K. Baranova, and I. V. Smolyar (2006), World ocean database 2005, S. Levitus Ed., NOAA Atlas NESDIS 60, Government Printing U. S. Office Washington, D.C., 190 pp., DVDs.

Clarke, A. J., and S. Van Gorder (2001), ENSO prediction using an ENSO trigger and a proxy for western equatorial Pacific warm pool movement, *Geophys. Res. Lett.*, *28*, 579–582.

Cronin, M. F., and M. J. McPhaden (2002), Barrier layer formation during westerly wind bursts, *J. Geophys. Res.*, *107*(C12), 8020, doi:10.1029/2001JC001171.

de Boyer Montégut, C., G. Madec, A. S. Fischer, A. Lazar, and D. Iudicone (2004), Mixed layer depth over the global ocean: An examination of profile data and a profile-based climatology, *J. Geophys. Res.*, *109*, C12003, doi:10.1029/2004JC002378.

Delcroix, T., and M. J. McPhaden (2002), Interannual sea surface salinity and temperature changes in the western Pacific warm pool during 1992–2000, *J. Geophys. Res.*, *107*(C12), 8002, doi:10.1029/2001JC000862.

Delcroix, T., and J. Picaut (1998), Zonal displacement of the western equatorial Pacific "fresh pool", *J. Geophys. Res.*, *103*, 1087–1098.

Delcroix, T., G. Eldin, M.-H. Radenac, J. Toole, and E. Firing (1992), Variation of the western equatorial Pacific Ocean, 1986–1988, *J. Geophys. Res.*, *97*, 5423–5445.

Delcroix, T., F. Baurand, G. Eldin, F. Gallois, Y. Gouriou, M. Rodier, and D. Varillon (2002), Rapport de la mission FRONTALIS à bord du Navire Océanographique l'Alis, 29 mars-26 avril 2001, 22°S–5°N/155°E–165°E, UMR LEGOS, Toulouse, *internal report*, 130 pp.

Eldin, G., M. Rodier, and M.-H. Radenac (1997), Physical and nutrient variability in the upper equatorial Pacific associated with westerly wind forcing and wave activity in October 1994, *Deep Sea Res.*, *44*, 1783–1800.

Eldin, G., T. Delcroix, and M. Rodier (2004), The frontal area at the eastern edge of the western equatorial Pacific warm pool in April 2001, *J. Geophys. Res.*, *109*, C07006, doi:10.1029/2003JC002088.

Eldin, G., M. Rodier, T. Delcroix, C. Maes, and R. Le Borgne (2005), The frontal zone at the eastern edge of the western tropical Pacific warm pool: Displacements and structure variability associated with in-

traseasonal forcing, *Dynamic Planet 2005*, Cairns, Australia, August 22–26.

Ganachaud, A., G. Eldin, R. Chuchla, M. Rodier, A. Lapetite, F. Gallois, and C. Dupouy (2006), Rapport de la mission FRONTALIS 2 à bord du N. O. Alis du 2 au 30 avril 2004, IRD Nouméa, *Rapports de Missions*, Sciences de la Mer, Océanographie Physique, No 18, 185 pp.

Godfrey, J. S., and E. J. Lindstrom (1989), The heat budget of the equatorial western Pacific surface mixed layer, *J. Geophys. Res.*, *94*, 8007–8017.

Godfrey, J. S., R. A. Houze Jr., R. H. Johnson, R. Lukas, J.-L. Redelsperger, A. Sumi, and R. Weller (1998), Coupled Ocean-Atmosphere Response Experiment (COARE): An interim report, *J. Geophys. Res.*, *103*, 14,395–14,450.

Huyer, A., P. M. Losro, R. Lukas, and P. Hacker (1997), Upper ocean thermohaline fields near 2°S, 156°E, during the tropical ocean-global atmosphere-coupled ocean-atmosphere response experiment, November 1992 to February 1993, *J. Geophys. Res.*, *102*(C6), 12,749–12,784.

Inoue, H. Y., M. M. Ishii, H. Matsueda, M. Ahoyama, and I. Asanuma (1996), Changes in longitudinal distribution of the partial pressure of CO_2 (pCO_2) in the central and western equatorial Pacific, west of 160°W, *Geophys. Res. Lett.*, *23*, 1781–1784.

Jackett, D. R., and T. J. McDougall (1995), Minimal adjustment of hydrographic profiles to achieve static stability, *J. Atmos. Oceanic Technol.*, *12*, 381–389.

Lagerloef, G. S. E. (2002), Introduction to the special section: The role of surface salinity on upper ocean dynamics, air-sea interaction and climate, *J. Geophys. Res.*, *107*(C12), 8000, doi:10.1029/2002JC001669.

Le Borgne, R., R. A. Feely, and D. J. Mackey (2002), Carbon fluxes in the equatorial Pacific: A synthesis of the JGOFS programme, *Deep Sea Res., II*, *49*, 2425–2442.

Lengaigne, M., J.-P. Boulanger, C. Menkes, S. Masson, G. Madec, and P. Delecluse (2002), Westerly wind event, *J. Geophys. Res.*, *107*(C12), 8015, doi:10.1029/2001JC000841.

Lindstrom, E., R. Lukas, R. Fine, E. Firing, S. Godfrey, G. Meyers, and M. Tsuchiya (1987), The western equatorial Pacific Ocean circulation study, *Nature*, *330*, 533–537.

Lukas, R., and E. Lindstrom (1991), The mixed layer of the western equatorial Pacific Ocean, *J. Geophys. Res.*, *96*(suppl), 3343–3357.

Maes, C., and D. Behringer (2000), Using satellite-derived sea level and temperature profiles for determining the salinity variability: A new approach, *J. Geophys. Res.*, *105*, 8537–8547.

Maes, C., P. Delecluse, and G. Madec (1998), Impact of westerly wind bursts on the warm pool of the TOGA-COARE domain in an OGCM, *Clim. Dyn.*, *14*, 55–70.

Maes, C., J. Picaut, and S. Belamari (2002), Salinity barrier layer and onset of El Niño in a Pacific coupled model, *Geophys. Res. Lett.*, *29*(24), 2206, doi:10.1029/2002GL016029.

Maes, C., J. Picaut, Y. Kuroda, and K. Ando (2004), Characteristics of the convergence zone at the eastern edge of the Pacific warm pool, *Geophys. Res. Lett.*, *31*, L11304, doi:10.1029/2004GL019867.

Maes, C., J. Picaut, and S. Belamari (2005), Importance of salinity barrier layer for the buildup of El Niño, *J. Clim.*, *18*, 104–118.

Maes, C., E. Kestenare, A. Ganachaud, F. Gallois, M. Rodier, D. Varillon, G. Eldin, R. Chuchla, and A. Lapetite (2006a), Rapport de la mission FRONTALIS 3 à bord du N. O. Alis du 22 avril au 19 mai 2005, 22°S–2°N/161°E–172°E, IRD Nouméa, *Rapports de Missions*, Sciences de la Mer, Océanographie Physique, No 20, 167 pp.

Maes, C., K. Ando, T. Delcroix, W. S. Kessler, M. J. McPhaden, and D. Roemmich (2006b), Observed correlation of surface salinity, temperature and barrier layer at the eastern edge of the western Pacific warm pool, *Geophys. Res. Lett.*, *33*, L06601, doi:10.1029/2005GL024772.

Matsumoto, K., K. Furuya, and T. Kawano (2004), Association of picophytoplankton distribution with ENSO events in the equatorial Pacific between 145°E and 160°W, *Deep Sea Res., I*, *51*, 1851–1871.

McDougall, T. J. (1987), Neutral surfaces, *J. Phys. Oceanogr.*, *17*, 1950–1964.

McPhaden, M. J., and J. Picaut (1990), El Niño-southern oscillation displacements of the western equatorial Pacific warm pool, *Science*, *250*, 1385–1388.

Murtugudde, R., and A. J. Busalacchi (1998), Salinity effects in a tropical ocean model, *J. Geophys. Res.*, *103*, 3283–3300.

Neelin, J. D., D. S. Battisti, A. C. Hirst, F.-F. Jin, Y. Wakata, T. Yamagata, and S. E. Zebiak (1998), ENSO theory, *J. Geophys Res.*, *103*, 14,261–14,290.

Picaut, J., M. Ioualalen, C. Menkes, T. Delcroix, and M. J. McPhaden (1996), Mechanism of the zonal displacements of the Pacific warm pool: Implications for ENSO, *Science*, *274*, 1486–1489.

Picaut, J., F. Masia, and Y. du Penhoat (1997), An advective-reflective conceptual model for the oscillatory nature of the ENSO, *Science*, *277*, 663–666.

Picaut, J., M. Ioualalen, T. Delcroix, F. Masia, R. Murtugudde, and J. Vialard (2001), The oceanic zone of convergence on the eastern edge of the Pacific warm pool: A synthesis of results and implications for ENSO and biogeochemical phenomena, *J. Geophys. Res.*, *106*, 2363–2386.

Richardson, R. A., I. Ginis, and L. M. Rothstein (1999), A numerical investigation of the local ocean response to westerly wind burst forcing in the western equatorial Pacific, *J. Phys. Oceanogr.*, *29*, 1334–1352.

Ridgway, K. R., and J. R. Dunn (2003), Mesoscale structure of the mean East Australian Current system and its relationship with topography, *Prog. Oceanogr.*, *56*, 189–222.

Rodier, M., G. Eldin, and R. Le Borgne (2000), The western boundary of the equatorial Pacific upwelling: Some consequences of climatic variability on hydrological and planktonic properties, *J. Oceanogr.*, *56*, 463–471.

Roemmich, D., M. Morris, W. R. Young, and J.-R. Donguy (1994), Fresh equatorial jets, *J. Phys. Oceanogr.*, *24*, 540–558.

Shinoda, T., H. H. Hendon, and J. Glick (1998), Intraseasonal variability of surface fluxes and sea surface temperature in the tropical western Pacific and Indian Oceans, *J. Clim.*, *11*, 1685–1702.

Sprintall, J., and M. Tomczak (1992), Evidence of the barrier layer in the surface layer of the Tropics, *J. Geophys. Res.*, *97*, 7305–7316.

Vialard, J., and P. Delecluse (1998), An OGCM study for the TOGA decade. Part I: Role of salinity in the physics of the western Pacific fresh pool, *J. Phys. Oceanogr.*, *28*, 1071–1088.

Vialard, J., P. Delecluse, and C. Menkes (2002), A modeling study of salinity variability and its effects in the tropical Pacific Ocean during the 1993–1999 period, *J. Geophys. Res.*, *107*(C12), 8005, doi:10.1029/2000JC000758.

Waliser, D. E. (1996), Formation and limiting mechanisms for very high sea surface temperature: Linking the dynamics and the thermodynamics, *J. Clim.*, *9*, 161–188.

Yoshida, K. (1959), A theory of the Cromwell current (the equatorial undercurrent) and of the equatorial upwelling-An interpretation in a similarity to a costal circulation, *J. Oceanogr. Soc. Jpn.*, *15*, 159–170.

You, Y. (1995), Salinity variability and its role in the barrier-layer formation during TOGA-COARE, *J. Phys. Oceanogr.*, *25*, 2778–2807.

C. Maes, Institut de Recherche pour le Développement (IRD), Laboratoire d'Etudes en Géophysique et Océanographie Spatiales (LEGOS), UMR065-IRD/CNES/CNRS/UPS, Centre IRD de Nouméa, B.P. A5, 98848 Nouméa cedex, New Caledonia. (maes@noumea.ird.nc)